Multifragmentation of $^{40}Ca + ^{40}Ca$

K. Hagel,[1] M. Gonin,[1],[a] R. Wada,[1] J. B. Natowitz,[1] B. H. Sa,[1],[b] Y. Lou,[1] M. Gui,[1] D. Utley,[1] G. Nebbia,[2] D. Fabris,[2] G. Prete,[2] J. Ruiz,[2] D. Drain,[3] B. Chambon,[3] B. Cheynis,[3] D. Guinet,[3] X. C. Hu,[3] A. Demeyer,[3] C. Pastor,[3] A. Giorni,[4] A. Lleres,[4] P. Stassi,[4] J. B. Viano,[4] and P. Gonthier[5]

[1]*Cyclotron Institute, Texas A&M University, College Station, Texas 77843*
[2]*Istituto Nazionale di Fisica Nucleare–Legnaro, I-35020, Legnaro, Italy*
[3]*Institut de Physique Nucléaire–Lyon, 69622 Villeurbanne CEDEX, France*
[4]*Institut des Science Nucléaires–Grenoble, 38026 Grenoble CEDEX, France*
[5]*Hope College, Holland, Michigan 49423*
(Received 12 November 1991)

The multifragment emission of "completely characterized" events in the $^{40}Ca + ^{40}Ca$ system at 35 MeV/nucleon has been compared to the predictions of several models. The observed multifragment emission is not in agreement with models based on conventional statistical binary decay, but is in agreement with both a simultaneous multifragmentation model and a sequential emission model in which expansion is treated.

PACS numbers: 25.70.Pq, 24.60.Dr, 25.70.Gh

The observation of multifragment emission following heavy ion collisions in the intermediate energy regime of 20 to 100 MeV/nucleon has been clearly established in numerous recent studies [1–5]. However, the dominant mechanism of multifragment emission has not yet been unambiguously determined. Standard equilibrium models which treat fragment emission as sequential binary decay from an equilibrated system predict an increase in the probability of sequential fragment emission with increasing excitation energy [6], as do formalisms which assume the simultaneous breakup of the system into multifragment final states [7,8]. We have studied the multifragment events in the $^{40}Ca + ^{40}Ca$ system at 35 MeV/nucleon in a nearly 4π configuration and have compared the experimental results to the predictions of various models. These comparisons indicate that the observed multifragment events result from hot nuclei which have undergone significant expansion.

In the experiment 35 MeV/nucleon ^{40}Ca ions were incident on a ^{40}Ca target in the AMPHORA [9] detector at the SARA Accelerator Facility . This detector consists of 120 CsI phoswich detectors that together cover 80% of 4π, 92 of which at angles less than 45° are covered by fast plastic detectors. To concentrate on central collisions, we recorded events only if a minimum of fourteen detectors fired. Hydrogen and helium isotopes were identified using pulse-shape discrimination. Heavier elements were identified with approximately unit Z resolution up to $Z=20$ using the ultrafast light component from the plastic and the slow component of the CsI. The energy calibration for protons was determined from the sharp cutoff in the energy spectrum which reflects the punchthrough energy. Energy calibrations for intermediate mass fragments (IMF's) were determined using the approximate beam velocity peaks in forward-angle spectra observed during a singles calibration run and determining quenching factors relative to the proton energies. The quenching factors deduced from the forward-angle spectra were used for all of the detectors. Uncertainties in the fragment energies are estimated to be $\pm 10\%$.

We have analyzed only events in which at least 90% of the total Z of the system was detected. These analyzed events are virtually complete, missing only a few particles (most likely very forward preequilibrium protons). The total energy of an event was calculated by summing the kinetic energies of all detected particles with the Q value and appropriate corrections for neutrons. We estimated the neutron contribution by assuming the same number of neutrons as protons and that their energies differ from the protons only by the Coulomb energy. Since our "complete" events are only about 1% of the total number of recorded events, accidental events where two reactions occur within the same beam burst could be emphasized. For these analyzed events, we estimate using a reaction simulation an accidental rate of 10% after restricting the total detected energy of an event to be less than 1500 MeV as well as demanding that particles be in the true time peaks in the time spectra. Further tests show that contamination by random events does not affect the results sufficiently to change the conclusions of this paper.

In the following we compare some of the experimental observables to the predictions of several statistical models. To make such comparisons, the mass (A) and excitation energy (E^*) of the deexciting system must be specified. At 35 MeV/nucleon, significant A and E^* may be removed by preequilibrium emission, even for very central collisions. For this symmetric system the experimental separation of preequilibrium and equilibrium emission from the particle spectra is difficult. We have therefore relied on several dynamic models to estimate the starting conditions of A, E^*, and, where applicable, angular momentum (J_{crit}) for the deexcitation calculation. Landau-Vlasov [10,11] and Boltzmann-Uehling-Uhlenbeck (BUU) [12,13] calculations indicate that at 35 MeV/nucleon the collision of $^{40}Ca + ^{40}Ca$ results in an initial compression followed by expansion. This takes about 70 fm/c. During this period significant preequilibrium emission occurs. Based on the calculations of Ref. [10], on BUU calculations using the codes of Refs. [12] and [13], and on preequilibrium emission estimates using the Boltzmann master equation [14] we have chosen $A=70$, $Z=34$, and $E^*=420$ MeV as the starting point of our calculations. The observables that we calculate do not change appreciably for reasonable ranges of initial mass and excitation energy.

All model calculations have been filtered through the same detection and analysis criteria as the experimental data. Differences between the calculations with and without the filter were found to be very small. To correct the Z distributions for the preequilibrium particles, which are not included in the calculation, we have added two protons to the Z distribution of each event. This brings the simulated total Z to the most probable total Z that was observed in our analyzed events.

We present in Fig. 1 the experimental charge distribution as solid points and the charge distributions predicted by several satistical models as histograms. The solid line represents the prediction of the simultaneous multifragmentation calculation of Sa and Gross [8] which assumes an expanded starting nucleus with $\rho \approx \frac{1}{6}\rho_0$. The dotted line is the prediction of the sequential binary decay model of Richert and Wagner [15], and the dashed line is the prediction of the statistical code GEMINI [6], which also treats the fragment emission as sequential. The J_{crit} for the latter has been chosen to be $60\hbar$ based on the estimate of the BUU calculation [13]. For the experimental events, we note a steep falloff in yield between $Z=1$ and 4, and then a more gradual decrease with increasing Z. Of the models considered in Fig. 1, the one which comes closest to describing the trend of this observed Z distribution is that of Sa and Gross. GEMINI produces the typical Z distribution expected from a normal statistical model, that is, a relatively large production of $Z=1$ and 2, a fairly low probability of fragments having $3 \leq Z \leq 15$, and a peak corresponding to heavy residues at higher Z. The sequential calculation of Richert and Wagner shows more IMF emission and a significant residue contribution at higher Z.

In Fig. 2 we show correlations between the fragment size and multiplicity. The figure shows the probability of detecting at least n fragments which have Z greater than or equal to a specified value which we call Z_{thresh}. The symbols represent the probabilities for $n=1,2,3,4$, etc. For the data shown in Fig. 2(a), we note that up to nine fragments having $Z \geq 3$ are observed. Figures 2(b)–2(d) show the predictions of the simultaneous multifragmentation model [8], the sequential binary code of Richert and Wagner [15], and the statistical model GEMINI [6], respectively. We note again that of these models the Sa-Gross model comes closest to reproducing the experimental data. The two standard sequential models show much

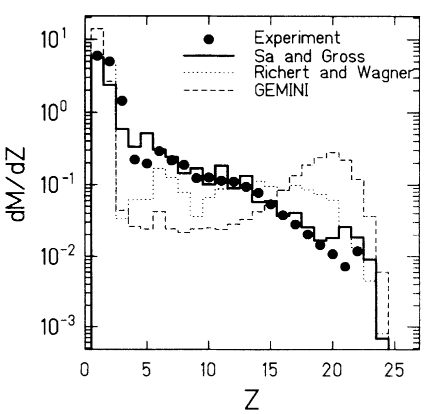

FIG. 1. Elemental charge distributions for the experiment and the model calculations. The points represent the data, the solid line represents the multifragmentation calculation of Sa and Gross, the dotted line represents the binary decay calculation of Richert and Wagner, and the dashed line represents the GEMINI calculation.

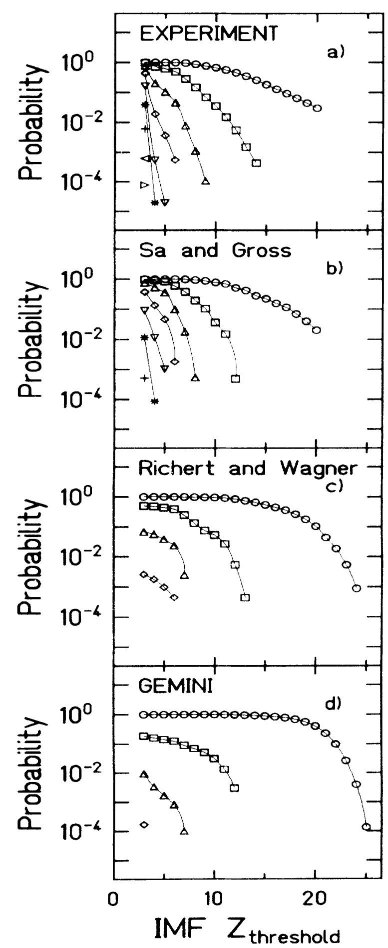

FIG. 2. Probability distributions for emission of at least n fragments, each having $Z \geq Z_{\text{thresh}}$. Symbols are $n=1$, ○; $n=2$, □; $n=3$, △; $n=4$, ◇; $n=5$, ▽; $n=6$, +; $n=8$, ◁; and $n=9$, ▷.

lower probabilities for multiple fragment emission than the multifragmentation model although the model of Richert and Wagner does predict slightly more than GEMINI.

Figure 3 shows the logarithmic distribution of the charge of the largest fragment per event versus the logarithm of the normalized second moment of the event charge distribution with the largest fragment excluded,

$$S_2' = \frac{\sum_{i:Z\neq Z_{\max}} Z_i^2 M(Z_i)}{\sum_{i:Z\neq Z_{\max}} Z_i M(Z_i)}.$$

Campi has suggested [16] that from such a plot it should be possible to determine which events result from simultaneous breakup of the system and which events result from the sequential decay of the system. Two peaks occur in the experimental contour plot in Fig. 3(a). One is located at large values of $\ln Z_{\max}$ and small values of $\ln S_2'$ and the other is located at small values of $\ln Z_{\max}$ and large values of $\ln S_2'$. Figure 3(b) shows the prediction of the multifragmentation code [8], 3(c) shows the prediction of the Richert and Wagner code [15], and 3(d) shows the prediction of GEMINI [6]. The multifragmentation calculation in Fig. 3(b) shows only one peak at large $\ln S_2'$ similar to the most prominent peak in Fig. 3(a). The other two calculations, on the other hand, show a large peak only at small values of $\ln S_2'$. These calculated peaks are at lower $\ln S_2'$ values than the peak at lower $\ln S_2'$ in the experimental data, a fact which reflects the dominance of light particle emission in the calculations.

The comparisons of Figs. 1–3 suggest that "normal" statistical models are not in agreement with the observations. Since expansion is a key ingredient in the reasonably successful simultaneous multifragmentation model, it is of interest to ask how sequential decay from an expanding system compares with the data. Friedman has proposed a sequential decay model in which the deexcitation of an expanding nucleus is treated [17]. In Fig. 4 we present for the schematic model of Friedman, with

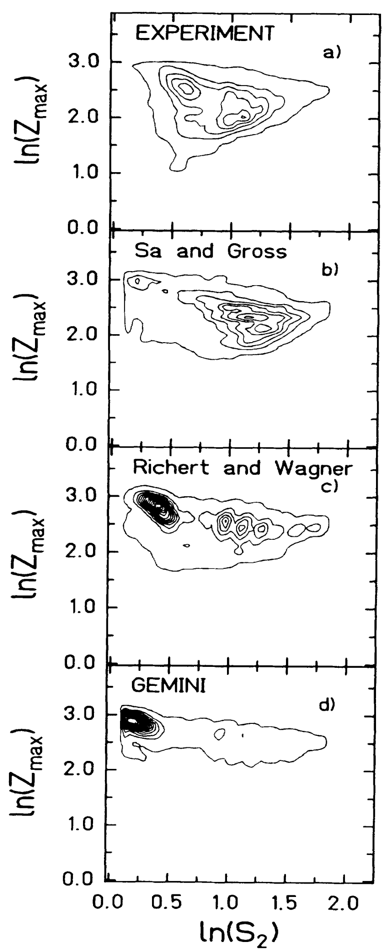

FIG. 3. Logarithmic distribution of $Z_{\max}$ vs S_2 (see text). Each contour represents a constant value in units of relative $d^2Y/d\ln S_2' d\ln Z_{\max}$, where Y is the yield. The outside contour is at a level of 10, and each inner contour represents a progressive increase in yield of 150. (a) Experiment, (b) multifragmentation calculation of Sa and Gross, (c) binary decay calculation of Richert and Wagner, and (d) GEMINI calculation.

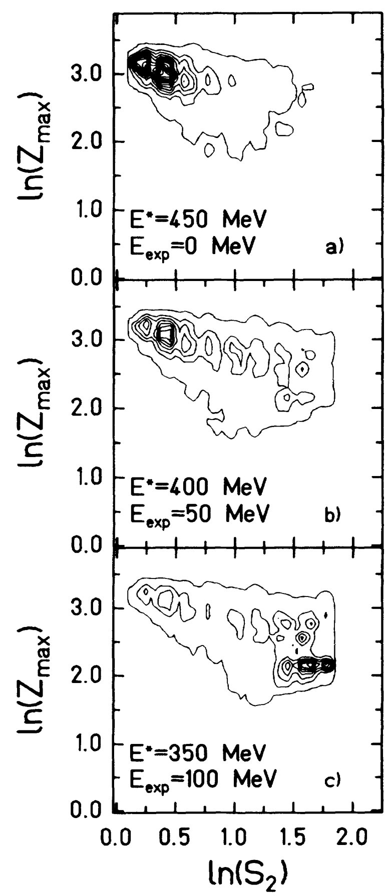

FIG. 4. Same as Fig. 3 for the schematic model of Friedman having E_{expan} of (a) 0 MeV, (b) 50 MeV, and (c) 100 MeV.

different assumed values of the expansion energy ($E_{\rm expan}$) of the deexciting system, plots like those of Fig. 3. When $E_{\rm expan}=0$, as shown in Fig. 4(a), the results are qualitatively similar to the GEMINI prediction. However, if $E_{\rm expan}=50$ or 100 MeV, as shown in Figs. 4(b) and 4(c), respectively, the distributions evolve toward larger values of $\ln S_2'$ and smaller values of $\ln Z_{\max}$. For $E_{\rm expan}=100$ MeV, the results shown in Fig. 4(c) are similar to those of the multifragmentation model presented in Fig. 3(b).

The minimum density reached in the model calculation which corresponds to Fig. 3(c) is about $\frac{1}{3}\rho_0$. This may be compared to the value of $\frac{1}{6}\rho_0$ used in the simultaneous multifragmentation calculation. At 35 MeV/nucleon the Landau-Vlasov and BUU codes lead to a minimum density near $\frac{1}{2}\rho_0$ [10–13]. It has been pointed out that at such low density the system enters the spinodal region and is subject to mechanical instabilities which could lead to multifragmentation [10,11,18]. Some expansion was also necessary to explain the results of Ref. [5].

In conclusion, we have experimentally isolated a set of "completely characterized" multifragmentation events. Model comparisons indicate that calculations which assume significant expansion of the deexciting system, such as the Sa and Gross simultaneous multifragmentation model or the expanding sequential decay model of Friedman, are in much better agreement with the observed behavior than are calculations with more standard sequential models. A characteristic of the Friedman model is that the bulk of the IMF emission, though sequential, occurs in a very short time scale at large expansion. We take the success of the two models incorporating expansion as a strong argument that the experimental events reflect the deexcitation from a hot expanded system rather than the equilibrium decay of a hot nucleus of normal density. The reasonable success of the two models does not presently allow a distinction to be made between simultaneous and sequential emission.

We thank W. M. Friedman, H. Xu, K. Niita, E. Suraud, and M. Blann for helpful discussions and for making their calculations available. We thank the staff of the SARA Accelerator Facility for their excellent support during the run. This work was supported by the U.S. Department of Energy under Grant No. DE-FG05-86ER40256, the National Science Foundation, the Robert A. Welch Foundation, and the Centre National de Recherche Scientifique.

(a)Present address: Brookhaven National Laboratory, Upton, NY 11973.

(b)Present address: Institute of Atomic Energy, Beijing, China.

[1] W. Mittig *et al.*, Phys. Lett. **154B**, 259 (1985).

[2] K. Hagel *et al.*, Phys. Lett. B **229**, 20 (1989).

[3] R. Bougault *et al.*, Phys. Lett. B **232**, 291 (1989).

[4] R. Bougault *et al.*, in Proceedings of the Twenty-Eighth Winter Meeting on Nuclear Physics, Bormio, Italy, 1990 (to be published).

[5] D. R. Bowman *et al.*, Phys. Rev. Lett. **67**, 1527 (1991).

[6] R. J. Charity *et al.*, Nucl. Phys. **A483**, 371 (1988).

[7] J. P. Bondorf *et al.*, Nucl. Phys. **A443**, 321 (1985).

[8] Sa Ban-Hao and D. H. E. Gross, Nucl. Phys. **A437**, 643 (1985); Xiao-Ze Zhang *et al.*, Nucl. Phys. **A461**, 641 (1987); Xiao-Ze Zhang *et al.*, Nucl. Phys. **A461**, 668 (1987).

[9] D. Drain *et al.*, Nucl. Instrum. Methods Phys. Res., Sect. A **281**, 528 (1989).

[10] K. Sneppen and L. Vinet, Nucl. Phys. **A480**, 342 (1988).

[11] E. Suraud, in *Proceedings of the Symposium on Nuclear Dynamics and Nuclear Disassembly*, edited by J. B. Natowitz (World Scientific, Singapore, 1989), p. 464.

[12] K. Niita *et al.*, Nucl. Phys. **A504**, 391 (1989).

[13] H. M. Xu *et al.*, Phys. Rev. Lett. **65**, 843 (1990).

[14] M. Blann, Phys. Rev. C **31**, 1245 (1985).

[15] J. Richert and P. Wagner, Nucl. Phys. **A517**, 399 (1990).

[16] X. Campi, J. Phys. A **19**, L917 (1986).

[17] W. Friedman, in Proceedings of the International Symposium on Nuclear Dynamics, Niiko, Japan, 1991 (AIP, New York, to be published), W. Friedman, Phys. Rev. Lett. **60**, 2125 (1988); Phys. Rev. C **42**, 667 (1990).

[18] Ch. J. Pethick and D. G. Ravenhall, Nucl. Phys. **A471**, 19c (1987).